Analyzing the wire scatterer using the method of moments with the step basis functions

Tuan Phuong Dang
Department of Television and Control
Tomsk State University of Control Systems and Radioelectronics
Tomsk, Russia
dang.p.2213-2023@e.tusur.ru

Adnan F. Alhaj Hasan
Department of Television and Control
Tomsk State University of Control Systems and Radioelectronics
Tomsk, Russia
alkhadzh@tusur.ru

Talgat R. Gazizov
Department of Television and Control
Tomsk State University of Control Systems and Radioelectronics
Tomsk, Russia
talgat.r.gazizov@tusur.ru

***Abstract*—This paper presents the development of an algorithmic mathematical model that uses the method of moments with step basis functions, an explanation of its mathematical formulation, and the development of a computer code based on it for modeling straight scatterer wires. The following scattering characteristics are considered: current distribution (magnitude and phase), radar cross section and back scattering cross section. These results were compared with those published in other papers and obtained numerically with triangular and sinusoidal basis functions, analytically and experimentally. A good agreement between the compared results is shown and the possibility of using the developed code to analyze wire scatterer structures is demonstrated.**

Keywords—scatterer, radar cross section, back scattering cross section, wire grid, method of moments.

I. INTRODUCTION

The development of new scattering structures has been of interest for a long time [1–4]. Currently, special attention is also paid to the study of wire scatterers and scattering structures based on them. Such studies have mainly consisted of the theoretical and experimental investigation of the radar cross section (RCS) and the back scattering cross section [5–7]. The earlier and current investigations were caried out using different numerical methods, but one of the most used method for modelling wire scatterers is the method of moments (MoM) [8, 9]. Researchers with the help of MoM investigated wire scatterers regarding to: arbitrary excitation and loading [10], arbitrary shape [11, 12], bent wires with junctions [13], developing new modelling algorithms [14, 15] and computer programs based on them [16, 17], frequency and time domains [18, 19].

In general, researchers used MoM with different basis functions such as triangular [13, 16] or sinusoidal [20] ones. But when dealing with these types of basis functions, there are difficulties in constructing their vertices at the node ends of the wire segments (one need to choose an appropriate number of segments to satisfy the conditions of segments and basis functions numbers), as well as at the intersection (junction) of wires [13, 16, 21].

On the other hand, the use of MoM with step basis functions seems to be easier in implementation and in segmentation of the wire structure (especially wires with junctions). Although these functions have disadvantages related to the convergence of the results, which may also require large computational resources, they have a remarkable advantage related to the formation of the MoM impedance matrix of the resulting system of linear equations. Eliminating one segment from the wire structure results in the elimination of only the matrix column and row corresponding to that segment. In other words, the existence of each individual segment is independent of the others (unlike the case with basis functions such as those constructed using points along the wire, like the triangular ones). This may allow us to utilize this advantage in the design of sparse wire grid scatterer structures [22]. Therefore, it is reasonably to use MoM with step basis functions to analyze scattering wire structures and more particularly those with complex shapes. Moreover, it is necessary to develop new mathematical models and program codes on their base to model such scattering wire structures.

In the classical work of Harrington [8], a general formulation for analyzing arbitrary wires using MoM was provided. However, to the best of our knowledge, the explanation and the realization of this formulation has not been made earlier based on using MoM with step basis functions and Dirac delta functions as testing ones. Moreover, among the well-known free and commercial computer codes, the step basis functions have not been used before for analyzing wire scatterers.

The aim of this paper is to develop an algorithmic mathematical model that uses MoM with step basis functions and a program code on its base to model straight scatterer wires. The results obtained in this study using Matlab code with the step basis functions were compared with those obtained numerically with triangular [10] and sinusoidal [20] basis functions, analytically [23] and experimentally [24].

This paper is organized as follows: Section II provides a comprehensive explanation of the formulas used in forming an algorithmic mathematical model for calculating and analyzing straight wire scatterers excited by plane waves. In addition, for solving such problem a simple formulation for setting the incident plane wave and forming appropriate excitation matrix was proposed. Section III presents the algorithmic mathematical model in a simple sequence of steps that enable designing a program on its base to calculate the components of the scattered field produced by the currents along straight wire. In Section IV, the results of modeling a straight scatterer wire using the developed Matlab code were compared with those published. Finally, Section V summarizes the research results and conclusions.

II. HISTORY: FORMULATION EXPLANATION

To explain the general formulation for analyzing arbitrary wires using MoM from [8], the same example of a scatterer wire with the length of L and radius of a (where $L>>a$) (Fig. 1)

This research was funded by the Ministry of Science and Higher Education of the Russian Federation project FEWM-2023-0014.

is considered. The analysis consists of the following. At first the wire should be divided into N segments.

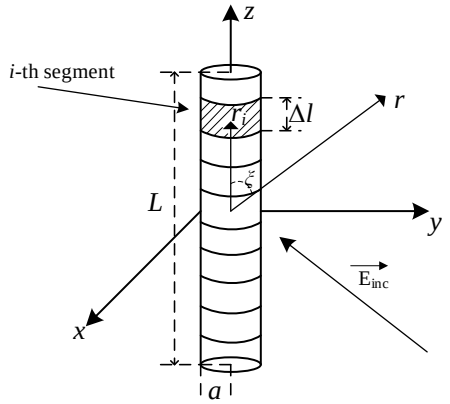

Fig. 1. The straight wire structure

One should note that N depends on the wavelength λ of the operating frequency (antenna problem) or the incident wave (scattering problem). In most cases, the segment length (Δl_i where i=1, …, N) should be less than λ/10, and in the case of complicate structures Δl_i<λ/20 but not less than λ/10000. It is reasonable that increasing N (or decreasing Δl_i) will increase the calculations accuracy, but this is valid as the $\Delta l_i/a$ ratio is bigger than 5. Moreover, increasing N will increase the number of operations, which leads to an increase in the required computational costs to solve the problem.

The step function (Fig. 2) has constant value in the segment and equal to zero outside it. The considered domain may be divided into N segments (pulses) with N+1 points Then, the step function is defined as:

$$f_j(x)=\begin{cases}1, & x_j \le x \le x_{j+1} \text{ where } j=1, \ldots, N+1,\\ 0, & \text{elsewhere.}\end{cases} \quad (1)$$

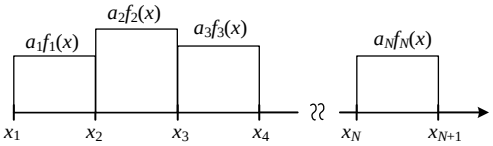

Fig. 2. The step basis functions.

When analyzing the scattering problem, the wire is excited by an external incident electric field $E^{inc}(i)$ where i=1, …, N is the segment index. According to [8] the voltage excitation matrix $[V^{inc}]$ can be calculated as

$$[V^{inc}]=\begin{bmatrix} E^{inc}(1)\Delta l_1 \\ E^{inc}(2)\Delta l_2 \\ \ldots \\ E^{inc}(N)\Delta l_N \end{bmatrix}. \quad (2)$$

When using MoM with step basis function, Δl_i value in (2) will be equal to the length of i-th segment. Then the unit plane wave will have the form [8]

$$E^{inc}=u_{inc}e^{-jk\vec{r}_i} \quad (3)$$

where k is the wave number vector pointing in the travel direction of the wave, $\vec{r}_i$ is the radius vector from the origin of the Cartesian coordinate system to the center of the i-th segment, u_{inc} is a unit vector specifying the polarization of the wave.

In [8], the formulation of the incident plane wave assignment and excitation matrix formation was not presented or explained directly for these types of basis functions. However, in this work the following simple representation is derived and used for the considered problem.

The unit plane wave in spherical coordinate for each element in the voltage excitation matrix can be written as

$$E^{inc}(i)=(\vec{n}_{seg}^{\,\theta}E_{\theta}^{inc}+\vec{n}_{seg}^{\,\varphi}E_{\varphi}^{inc})e^{-jk\vec{r}_i} \quad (4)$$

where E_{θ}^{inc} and E_{φ}^{inc} are the components of the incident electromagnetic wave according to the azimuthal θ^{inc} and elevation φ^{inc} angles that determine the direction of the wave.

As is known, when converting from the Cartesian to the spherical coordinate system, one should use the local orthogonal unit vectors in the directions of increment r, θ, and φ that given by:

$$\hat{r}=x\sin\theta\cos\varphi+y\sin\theta\sin\varphi+\hat{z}\cos\theta, \quad (5)$$

$$\theta=x\cos\theta\cos\varphi+y\cos\theta\sin\varphi-\hat{z}\sin\theta, \quad (6)$$

$$\varphi=-x\sin\varphi+y\cos\varphi \quad (7)$$

where φ, θ are the azimuthal and elevation angles in the spherical coordinate system, and $\hat{x}$, $\hat{y}$, $\hat{z}$ are the unit vectors in the Cartesian coordinate system. Then, the unit vectors of the considered segment: $\vec{n}_{seg}^{\,\theta}$ and $\vec{n}_{seg}^{\,\varphi}$ by θ^{inc} and φ^{inc} in the spherical coordinate system, can be written as:

$$\vec{n}_{seg}^{\,\theta}=\vec{n}_{segX}\cos\theta^{inc}\cos\varphi^{inc}+\vec{n}_{segY}\cos\theta^{inc}\sin\varphi^{inc}-\vec{n}_{segZ}\sin\theta^{inc}, \quad (8)$$

$$\vec{n}_{seg}^{\,\varphi}=-\vec{n}_{segX}\sin\varphi^{inc}+\vec{n}_{segY}\cos\varphi^{inc} \quad (9)$$

where $\vec{n}_{seg(X,\,Y,\,Z)}$ are the unit vector projections in the Cartesian coordinate system and have the following form:

$$\begin{aligned}\vec{n}_{segX}&=\Delta l_X/\Delta l,\\ \vec{n}_{segY}&=\Delta l_Y/\Delta l,\\ \vec{n}_{segZ}&=\Delta l_Z/\Delta l\end{aligned} \quad (10)$$

where Δl_X, Δl_Y, Δl_Z are the vector projection of the vector $\overrightarrow{\Delta l}$ (which has the direction from the segment start to end points) on the Cartesian coordinate system axis.

The phase of the excitation incident wave can be represented as:

$$k\vec{r}_i=k(x_{seg}^{center}\sin\theta^{inc}\cos\varphi^{inc}+y_{seg}^{center}\sin\theta^{inc}\sin\varphi^{inc}+z_{seg}^{center}\cos\theta^{inc}) \quad (11)$$

where $(x,\,y,\,z)_{seg}^{center}$ are the center coordinates of the considered segment.

According to [8], the impedance matrix $[Z]$ elements can be obtained by calculating the impedances (Z_{mn}) between each two segments (m and n) which requires the evaluation of the following scalar function (More details can be found in [8]):

$$\psi(n,m)=\frac{1}{\Delta l_n}\int_{\Delta l_n}\frac{e^{-jkR_{mn}}}{4\pi R_{mn}}dl_n \quad (12)$$

where Δl_n is the length of the n-th segment, R_{mn} is the distance between two points on the considered segments (Fig. 3), and it is given by:

$$R_{mn} = \begin{cases} \sqrt{\rho^2 + (z - z')^2}, & m \neq n, \\ \sqrt{a^2 + (z')^2}, & m = n \end{cases} \quad (13)$$

where the value of z is determined as the projection of the vector $\vec{z}$ between two points on each n and m segments on the vector of the n (or m) segment, through their scalar product

$$z = \frac{\vec{z}.\vec{n}}{\left|\vec{n}\right|}. \quad (14)$$

The value ρ is obtained by

$$\rho = \sqrt{r^2 - z^2}, \quad (15)$$

when $\rho<a$, then $\rho=a$. The distance r between two points on each n and m segments, which is equal to $\left|\vec{z}\right|$, is calculated by

$$r = \sqrt{(x_m - x_n)^2 + (y_m - y_n)^2 + (z_m - z_n)^2} \quad (16)$$

where $(x, y, z)_{mn}$ are the coordinates of the points on each m and n segments, respectively.

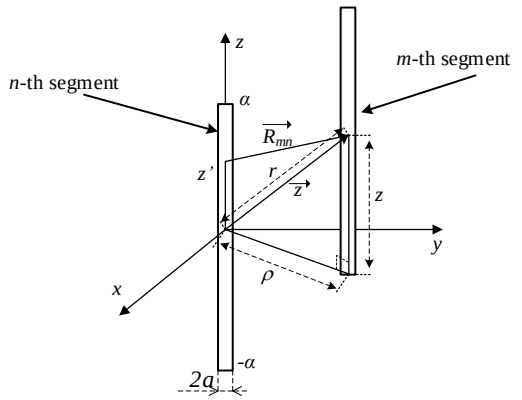

Fig. 3. The geometry for calculating ψ_{mn}

Then the impedance matrix element can be calculated as

$$Z_{mn} = j\omega\mu\Delta l_n \Delta l_m \psi(n,m) + \cdots + \frac{\psi(n^+,m^+) - \psi(n^-,m^+) - \psi(n^+,m^-) + \psi(n^-,m^-)}{j\varepsilon\omega} \quad (17)$$

where μ and ε are the medium absolute permeability and permittivity, while the symbols + and – are used over the segments m and n when appropriate to determine their start and end points. The product $\Delta l_n \Delta l_m$ can be obtained by:

$$\Delta l_n \Delta l_m = \Delta l_m^x \Delta l_n^x + \Delta l_m^y \Delta l_n^y + \Delta l_m^z \Delta l_n^z \quad (18)$$

where $\Delta l_{n,m}^{(x,y,z)}$ are the vector projection of the vectors $\overrightarrow{\Delta l}_n$ and $\overrightarrow{\Delta l}_m$ (that have the direction from the start to end points of the n, m segments, respectively) on the Cartesian coordinate system axis.

After fillings the impedance [Z] and the voltage [V] matrices one can find the elements of the current matrix [I] by solving the formed system of linear algebraic equations [Z][I]=[V^{inc}] using the multiplication of the matrix inverse [Z^{-1}] by [V^{inc}] as

$$[I] = [Z^{-1}][V^{inc}]. \quad (19)$$

As the current matrix elements are obtained, one can determine the electrical field intensity of the scattered field in the far zone by treating the wire as an array of N current elements $I_i \Delta l_i$ as

$$E^s = \frac{\mu\omega e^{-jkr}}{j4\pi r} \sum_0^N I_i \Delta l_i e^{jkr_i \cos\xi_i}. \quad (20)$$

To calculate (20), one may treat it as two independent and sequential parts: the phase and the amplitude (without the coefficient part). First, one should find the phase part γ as

$$\gamma_i = kr_i \cos\xi_i + \varphi_{Ii} \quad (21)$$

where φ_{Ii} is the current phase of the i-th segment, ξ_i is the angle between the vector $\vec{r}_i$ and the vector $\vec{r}$ – vector from the origin of the coordinate system to the point where the electrical field intensity is being calculated, and the unknown in (21) can be calculated using the scalar product of $\vec{r}$ and $\vec{r}_i$ as

$$r_i \cos\xi = \frac{\vec{r}.\vec{r}_i}{\left|\vec{r}\right|}. \quad (22)$$

Then, one may calculate the amplitude part as

$$A_{i(x,y,z)} = \left|I_i\right| \Delta l_{i(x,y,z)} \quad (23)$$

where $\Delta l_{i(x, y, z)}$ are the vector projections of the vector $\overrightarrow{\Delta l}_i$ on the Cartesian coordinate system axis.

Then the far field component along the axis of the Cartesian coordinate system from (20) can be written as

$$E^s{}_{(x,y,z)} = \frac{\mu\omega e^{-jkr}}{j4\pi r} \sum_0^N A_{i(x,y,z)} e^{j\gamma_i} \quad (24)$$

Then, the field components in the spherical coordinate system can be obtained as:

$$E_\theta^s = E_x^s \cos\theta\cos\varphi + E_y^s \cos\theta\sin\varphi - E_z^s \sin\theta, \quad (25)$$

$$E_\varphi^s = -E_x^s \sin\varphi + E_y^s \cos\varphi. \quad (26)$$

Finally, the total field in the far zone is given by

$$E_{total}^s = \sqrt{\left|E_\theta^s\right|^2 + \left|E_\varphi^s\right|^2}. \quad (27)$$

The bistatic RCS (σ) might be calculated as

$$\sigma_{(x,y,z)} = \frac{\eta^2 k^2}{4\pi} \left| \sum_0^N A_{i(x,y,z)} e^{j\gamma_i} \right|^2 \quad (28)$$

where $\eta = \sqrt{\mu/\varepsilon}$ is the impedance of free space. The σ components (in the spherical coordinate system) and their total can be obtained as

$$\sigma_\theta = \sigma_x \cos\theta\cos\varphi + \sigma_y \cos\theta\sin\varphi - \sigma_z \sin\theta, \quad (29)$$

$$\sigma_\varphi = -\sigma_x \sin\varphi + \sigma_y \cos\varphi, \quad (30)$$

$$\sigma_{total} = \sqrt{\left|\sigma_\theta\right|^2 + \left|\sigma_\varphi\right|^2}. \quad (31)$$

III. Algorithm Development

Based on the provided, modernized and explained mathematical model, an algorithm for analyzing wire scatterer using MoM with step basis functions and calculating its bistatic RCS is developed and presented further.

1. Creation of the scatterer geometric model

1.1. Set the parameters of the scatterer wire: its radius and its start and end points coordinates.

1.2. Set the number of segments on which the wire will be divided.
1.3. Determine the start, end and center points coordinates of each segment along the wire.
1.4. Calculate the length of each segment Δl_i.
2. *Calculation of the voltage excitation matrix*
2.1. Set the parameters of the incident plane wave: frequency; amplitudes of the E_θ^{inc} and E_φ^{inc} components; the angles θ^{inc} and φ^{inc} that define the wave direction.
2.2. Calculate the wavenumber and then the unit plane wave $E^{inc}(i)$ in spherical coordinate for each element in the voltage excitation matrix using the following formulas in sequence: (10), (8), (9), (11), and then (4).
2.3. Fill the voltage excitation matrix $[V^{inc}]$ as in (2) with the obtained results from 1.4 and 2.2.
3. *Calculation of impedance matrix*
3.1. Set the values of the medium μ and ε.
3.2. Calculate the vector $\vec{z}$ between two points on each two segments and its projections z on the each considered segment by (14).
3.3. Calculate the distance r between two points on each two segments by (16).
3.4. Calculate ρ by (15) using the obtained results from 3.2 and 3.3.
3.5. Calculate the value of α as half-length of each segment.
3.6. Calculate the scalar functions ψ^{++}, ψ^{+-}, ψ^{-+}, ψ^{--}, ψ of each two segments as in [8, 25] using the obtained results from 3.2–3.5.
3.7. Calculate the scalar product of the $\overrightarrow{\Delta l}_n$ and $\overrightarrow{\Delta l}_m$ vectors of each two n and m segments using (18).
3.8. Calculate the impedance matrix elements by (17) using the result from 3.6 and 3.7.
4. *Calculation of the current matrix*
4.1. Find the elements of the current matrix $[I]$ through the matrix multiplication of $[Z^{-1}]$ by $[V^{inc}]$ (19).
5. *Calculation of the scattered field in the far–zone*
5.1. Set the spherical coordinate components (azimuthal φ and elevation θ angles and r) required to determine the points in the far field where the field intensity will be calculated.
5.2. Calculate the phase part γ_i using (22) and then (21), and the amplitude part $A_{i(x,y,z)}$ using (23).
5.3. Calculate the coefficient $\frac{\mu\omega e^{-jkr}}{j4\pi r}$ in (20).
5.4. Calculate the scattered field components in the Cartesian coordinate system using (24).
5.5. Convert the scattered field components from the Cartesian to the spherical coordinate system using (25)–(27).
5.6. Calculate η and the bistatic RCS components in the Cartesian coordinate system using (28).
5.7. Convert the bistatic RCS components from the Cartesian to the spherical coordinate system (29)–(31).

IV. Numerical results

Based on the developed algorithm in the previous section, a Matlab code was written to analyze straight scatterer wires. In order to verify the results of the developed program, its results were compared with the published ones of other researchers obtained for the same problem: numerically using triangular functions [10], numerically using sinusoidal functions [20], analytically [23] and experimentally [24]. The incident wave in all considered cases is a plane wave and has an amplitude of 1 V/m while the angle of incidence is different for each case.

First, we compared our results with those obtained in [10] using MoM with triangular functions and 32 segments. The authors of [10] considered two cases of scatterer wire: L=1.5λ and 2λ where $L/2a$=74.2. The incident plane wave is considered at different angles θ^{inc}=15, 30, 45, 60, 75, 90°. Here, we modeled the two cases with different segment numbers of 32, 64, and 90. The dependences of the current magnitude $|I|$ and phase φ_I on the coordinates along the wire for the two cases obtained in [10] and using Matlab are presented in Fig. 4, 5.

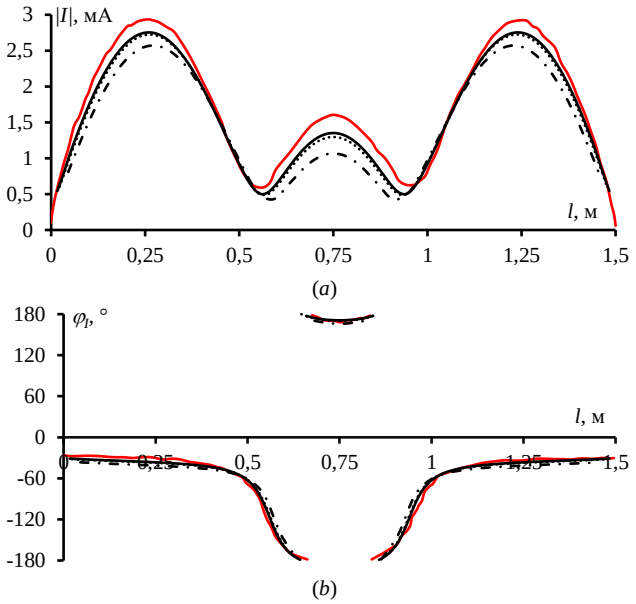

Fig. 4. The dependences of $|I|$ (*a*) and φ_I (*b*) on coordinates along the L=1.5λ wire with θ^{inc}=90°: [10] (—), Matlab using 32 (–·–), 64 (···) and 90 (—) step basis functions.

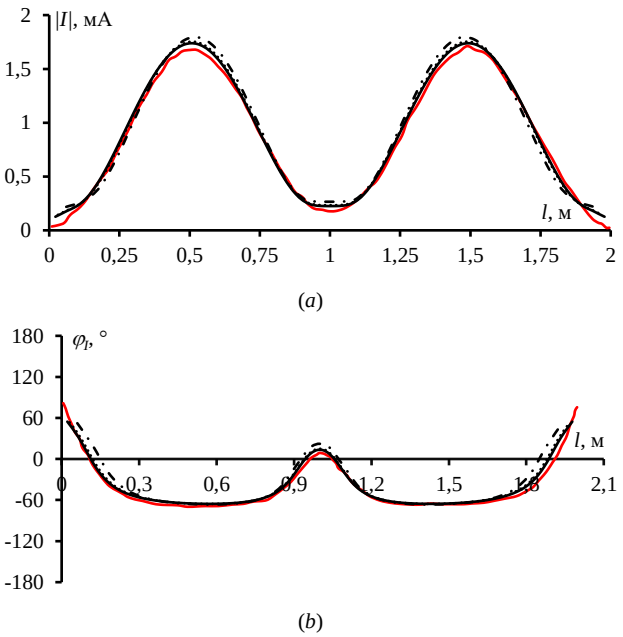

Fig. 5. The dependences of $|I|$ (*a*) and φ_I (*b*) on coordinates along the L=2λ wire with θ^{inc}=90°: [10] (—), Matlab using 32 (–·–), 64 (···) and 90 (—) step basis functions.

The maximum $|I|$ are calculated in Matlab using 90 segments and compared to those from [10] also for the two wire cases at different θ^{inc} and summarized in Table I.

TABLE I. THE MAXIMUM $|I|$ IN MA FOR THE TWO WIRE CASES AT DIFFERENT θ^{inc}

L, m	Model	θ^{inc}, °					
		15	30	45	60	75	90
1.5λ	Matlab	6.25	6.2	5.279	2.84	1.74	2.7
	[10]	6.95	6.78	5.68	2.99	1.85	2.9
	$\Delta\|I_{max}\|$, %	10.7	8.5	7.06	5.01	5.94	6.89
	$\Delta\varphi_I$, %	2.1	2.2	0.5	1.1	2.02	1.05
2λ	Matlab	8.07	7.5	4.94	2.223	2.866	1.78
	[10]	8.92	8.08	5.27	2.407	3.11	1.71
	$\Delta\|I_{max}\|$, %	9.5	6.8	6.3	7.6	7.8	3.9
	$\Delta\varphi_I$, %	1.5	1.56	2.47	1.7	0.81	3.03

Upon analyzing the results in Figs. 4 and 5 and Table I, one can notice that when using MoM with step basis functions, the maximum deviation of $|I_{max}|$ obtained in Matlab compared to those from [10] is about 11 %. The maximum deviation of φ_I in the segments corresponding to the considered $|I_{max}|$ is about 3 %.

Fig. 6 and 7 show the calculated RCS for the two wire cases at θ^{inc} of 45, 60, and 90° obtained in Matlab and from [10]. The obtained data show that the compared RCS are in good agreement with maximum deviation of 9% (Fig. 6*a*). One may notice that the angle of the main lobe of the scattering field is symmetric to the direction of the incident wave through the perpendicular plane to the plane that contains the wire, which is consistent with the mirror diffraction theory.

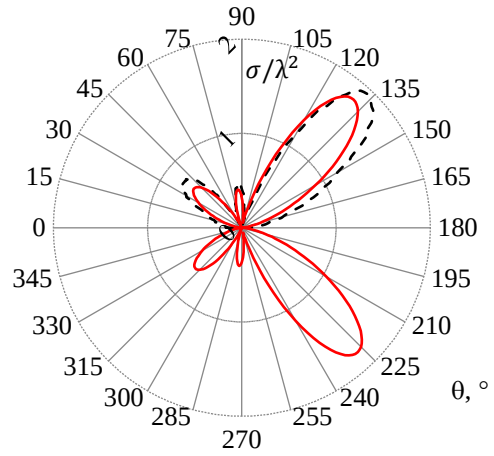

(*a*)

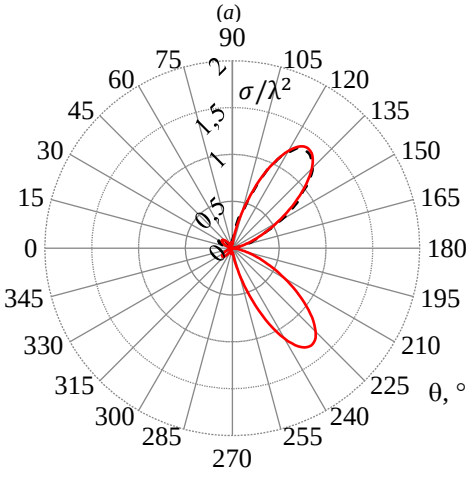

(*b*)

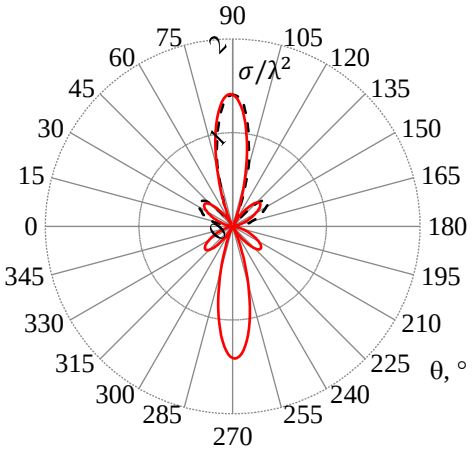

(*c*)

Fig. 6. The RCS of the L=1.5λ wire scatterer at θ^{inc} of 45° (*a*), 60° (*b*) and 90° (*c*) obtianed in [10] (– –) and in Matlab with 60 step basis functions (—)

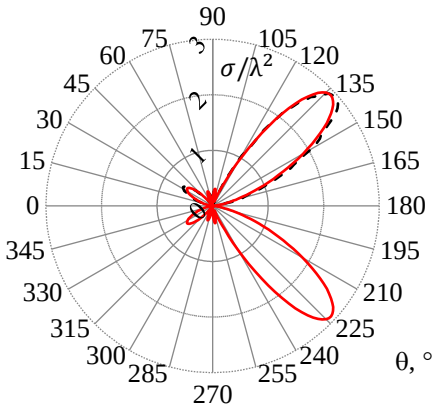

(*a*)

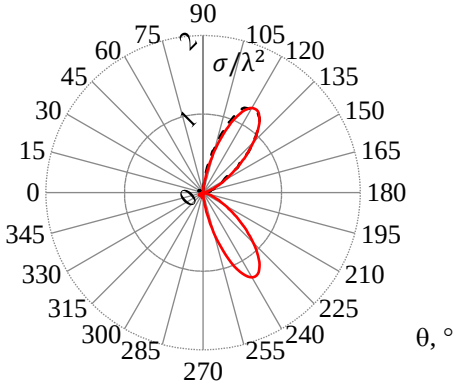

(*b*)

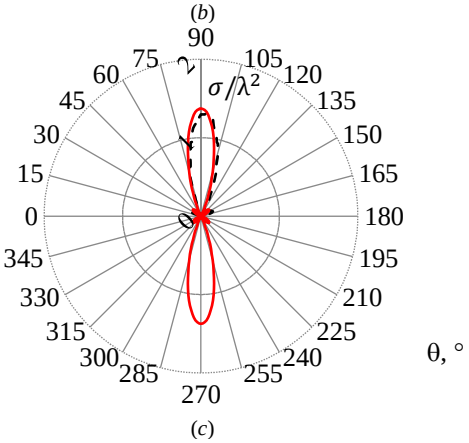

(*c*)

Fig. 7. The RCS of the L=2λ wire scatterer at θ^{inc} of 45° (*a*), 60° (*b*) and 90° (*c*) obtianed in [10] (– –) and in Matlab with 60 step basis functions (—).

Next, we considered the scatterer wire from [20], which modeled using basis sinusoidal function with 31 segments and with the following parameters: L=1.5λ, $2\pi a$=0.0635λ, θ^{inc}=30°. The dependences of $|I|$ and φ_I on coordinates along the wire and its RCS obtained in [20] and using Matlab are presented in Fig. 8 and 9. The results analysis shows that the compared $|I|$ values differ maximally by about 11%, and their φ_I differ by about 1%. The RCS values at the main lobe differ by about 11%.

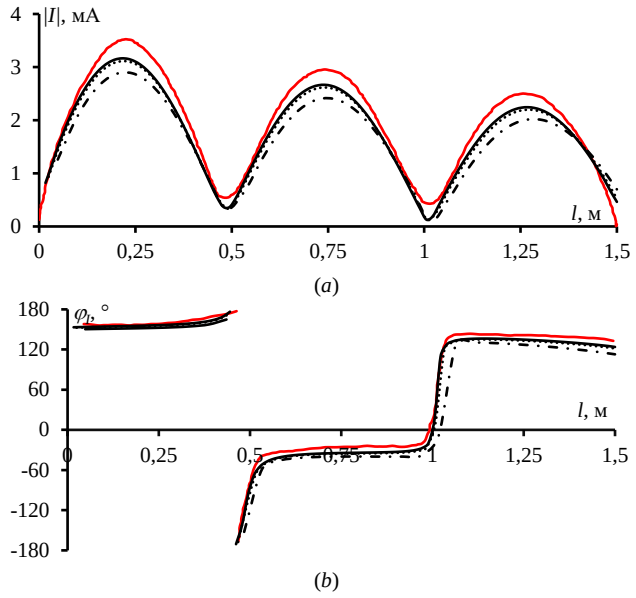

Fig. 8. The dependences of $|I|$ (*a*) and φ_I (*b*) on coordinates along the wire obtained in: [20] (–), Matlab with 31 (–·–), 61 (··), 91 (–) step basis functions.

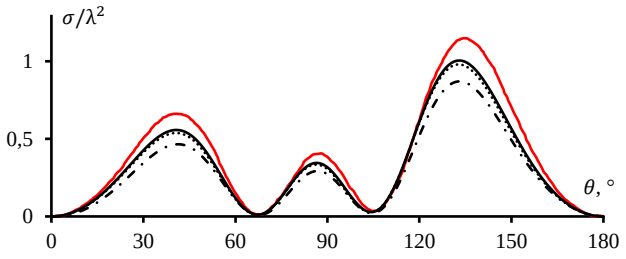

Fig. 9. The RCS of the scatterer wire obtained in: [20] (—), Matlab with 31 (–·–), 61 (···), 91 (—) step basis functions.

Then we considered the scatterer wire from [23] in two cases: L/λ=0.75, L/a=150 and L/λ=4.065, L/a=2856. The RCS for the two cases obtained analytically in [22] and using MoM with 64 step basis functions are compared in Fig. 10. The compared results were in good agreement. Plots of the long wires are bigger in magnitudes and have several minimums and maximums than those for short ones. In general, the RCS is larger as the wire length increases.

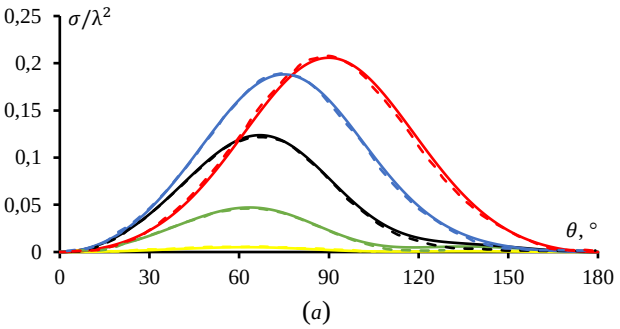

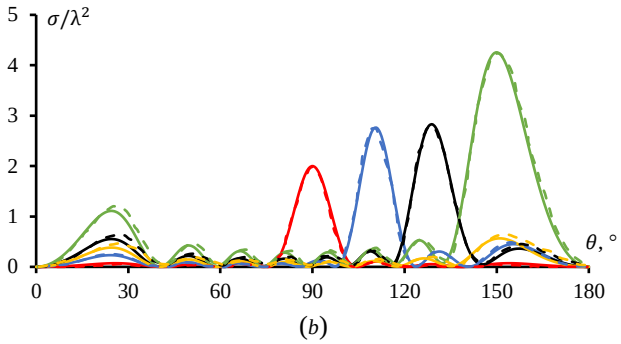

Fig. 10. The RCS for wire cases: L/λ=0.75 (*a*) and L/λ=4.065 (*b*), obtained at θ^{inc}=90°(red), 70°(blue), 50°(black), 30°(green), 10°(yellow), and using MoM with 64 segments (solid) and analytically in [23] (dashes).

Finally, we considered the scatterer wire form [24] where the dependences of the back scattering cross section on the L/λ ratio when varying the wire length from 0.1λ to 5.4λ (with a/λ=0.00627) were obtained experimentally. As well known, when the incident wave is perpendicular to the surface where the scatterer wire is located, the main lobe of the RCS will be in the opposite direction. Therefore, we will consider this case when calculating the backscattering cross section using MoM. The length of the segment is taken to be 5 times the wire radius. Fig. 11 compares the results obtained in [24] and using Matlab. The comparison shows that in general the compared results are in good agreement especially when the wire length is less than 4.5λ (with maximum deviation is about 8%). However, when the wire length is larger 4.5λ, the deviation increases up to 20%. Moreover, it can be noticed that in cases where the wire length is equal to an odd number of λ/2, the largest back scattering is obtained compared, which is completely consistent with the scattering theory.

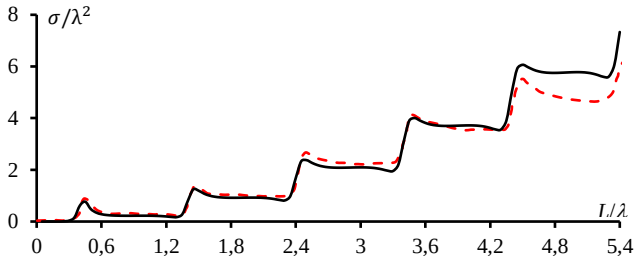

Fig. 11. The dependences of the back scattering cross section of the scatterer wire form [24] on the L/λ ratio: measured (– –) and calculated (—)

V. Conclusion

This paper provides a comprehensive comparative analysis of the scattering characteristics from straight wires. The main contributions include developing an algorithmic mathematical model that uses MoM with step basis functions and explaining its mathematical formulation so the researchers can easily develop a computer code on its base for modeling straight scatterer wires. A Matlab code was developed and used to model different scatterers from different works. The calculated using Matlab results were obtained and compared with those obtained numerically with triangular and sinusoidal basis functions, analytically and experimentally. The comparison showed a good agreement in the scattered electromagnetic field calculations which verifies our results. In addition, this demonstrates the possibility of using MoM with step basis function to analyze and simulate wire scatterer structures. In the future, the developed model and code can be used to analyze more complex wire structures and especially the sparse ones.

VI. REFERENCES

[1] M. A. Richards, T. H. Shumpert and L. S. Riggs, “A modal radar cross section of thin-wire targets via the singularity expansion method,” in IEEE Transactions on Antennas and Propagation, vol. 40, no. 10, pp. 1256–1260, Oct. 1992.

[2] R.C.J. Smets, “Electromagnetic excitation of a thin wire: an analytic approach”, Eindhoven University of Technology, Aug. 1994.

[3] C. Taylor, “Electromagnetic scattering from arbitrary configurations of wires,” in IEEE Transactions on Antennas and Propagation, vol. 17, no. 5, pp. 662–663, Sep. 1969.

[4] S. H. Dike and D. D. King, “The absorption gain and back-scattering cross section of the cylindrical antenna,” in Proceedings of the IRE, vol. 40, no. 7, pp. 853–860, July 1952.

[5] I. Kurtoglu and I. H. Cavdar, “Electromagnetic imaging of discrete wire scatterers via MUSIC algorithm: preliminary experimental results,” 2019 Seventh International Conference on Digital Information Processing and Communications (ICDIPC), Trabzon, Turkey, 2019, pp. 5–7.

[6] M. Stumpf, "Influence of a wire scatterer on a receiving wire antenna," in Time-Domain Electromagnetic Reciprocity in Antenna Modeling, IEEE, 2019, pp. 59–64.

[7] P. L. E. Uslenghi, “Scattering by two parallel metal wires over a conducting ground plane,” 2018 International Conference on Electromagnetics in Advanced Applications (ICEAA), Cartagena, Colombia, 2018, pp. 5–7.

[8] R. F. Harrington, “Matrix methods for field problems,” in Proceedings of the IEEE, vol. 55, no. 2, pp. 136–149, Feb. 1967.

[9] R. G. Harrington, and J. L. Harrington, “Field computation by moment methods”. Oxford University Press, Inc., 1996.

[10] R. Harrington and J. Mautz, “Straight wires with arbitrary excitation and loading,” in IEEE Transactions on Antennas and Propagation, vol. 15, no. 4, pp. 502–515, July 1967.

[11] D. X. Wang, K. N. Yung and R. S. Chen, “Efficient analysis of wire antennas and scatterers with arbitrary shape,” in IEEE Antennas and Wireless Propagation Letters, vol. 2, pp. 107–110, 2003.

[12] A. Kadhum, B. J. Hu and J. X. Yin, “Scattering analysis of arbitrarily shaped conducting thin wire structures,” in 2005 Asia-Pacific Microwave Conference Proceedings, Suzhou, China, vol. 3, 2001.

[13] H. Chao, B. Strait and C. Taylor, “Radiation and scattering by configurations of bent wires with junctions,” in IEEE Transactions on Antennas and Propagation, vol. 19, no. 5, pp. 701–702, Sep. 1971.

[14] A. Zhu, S. Gedney and K. W. Whites, “Point-based high-order moment method for thin wire scattering and antenna analysis,” in IEEE Antennas and Propagation Society International Symposium. 2001 Digest. Held in conjunction with: USNC/URSI National Radio Science Meeting (Cat. No.01CH37229), vol. 2, pp. 538–541, 2001.

[15] M. N. I. Fahmy and I. A. Eshrah, “Pseudo-exact simple closed-form solutions for radiation and scattering from thin straight loaded and unloaded wires,” in Proceedings of the Nineteenth National Radio Science Conference, pp. 109–124, Alexandria, Egypt, 2002.

[16] H. H. Chao, B. J. Strait, “Computer programs for radiation and scattering by arbitrary configurations of bent wires”. Syracuse, NewYork, Sep. 1970.

[17] J. H. Richmond, “Digital computer solutions of the rigorous equations for scattering problems,” in Proceedings of the IEEE, vol. 53, no. 8, pp. 796–804, Aug. 1965.

[18] J. H. Richmond, "Radiation and scattering by thin wire structures in the complex frequency domain,” Washington, D. C. May 1974.

[19] E. K. Miller and J. A. Landt, “Direct time-domain techniques for transient radiation and scattering from wires,” in Proceedings of the IEEE, vol. 68, no. 11, pp. 1396–1423, Nov. 1980.

[20] J. Scherer, “Computer programs for EMC based on the methods of moments”, Syracuse University, 1980.

[21] C. Butler, “Currents induced on a pair of skew crossed wires,” in IEEE Transactions on Antennas and Propagation, vol. 20, no. 6, pp. 731–736, Nov. 1972.

[22] A. Alhaj Hasan, T. M. Nguyen, S. P. Kuksenko and T. R. Gazizov, “Wire-grid and sparse MoM antennas: past evolution, present implementation and future possibilities,” Symmetry, vol. 15, no. 2, p. 378, Jan. 2023.

[23] K. Dedrick, A. Hessing and G. Johnson, “Bistatic radar scattering by randomly oriented wires,” in IEEE Transactions on Antennas and Propagation, vol. 26, no. 3, pp. 420–426, May 1978.

[24] V. V. Liepa and S. Chang, “Measured back scattering cross section of thin wires," IEEE Antennas and Propagation Society International Symposium. 1999 Digest. Held in conjunction with: USNC/URSI National Radio Science Meeting (Cat. No.99CH37010), Orlando, FL, USA, vol. 3, pp. 1980–1982, 1999.

[25] A. Alhaj Hasan, A.A. Kvasnikov, D.V. Klyukin, A.A. Ivanov, A.V. Demakov, D.M. Mochalov, S.P. Kuksenko, “On modeling antennas using mom-based algorithms: wire-grid versus surface triangulation,”Algorithms, vol. 16, no. 4. p. 200, 2023.